

Decoupling and Control of Real and Reactive Power in Grid-Connected Photovoltaic Power System

Tayeb Allaoui
Faculty of Engineering, L2GEGI Laboratory
University of Tiaret, Algeria
allaoui_tb@yahoo.fr

Mouloud Denai
School of Science and Engineering
Teesside University, UK
m.denai@tees.ac.uk

Abstract—The paper presents a detailed modeling and simulation of different control schemes of the real and reactive power flows in a three-phase voltage source inverter (VSI) interfacing a photovoltaic (PV) generation system to the power grid. Synchronisation of the inverter and grid AC waveforms is achieved using a phase-locked-loop (PLL) circuit. An effective decoupling strategy based on proportional-integral (PI) controllers is designed to eliminate the interaction between the two current components. Finally, the influence of the grid disturbances on the PV system and the influence of the solar energy intermittency on the power grid have been tested. The overall model is implemented in Matlab and Simulink/SimPowerSystems toolboxes. Simulations results with the PV system operating with real irradiance data will be presented to demonstrate the performance of the proposed decoupling and control strategies under different conditions of the power grid.

Keywords—Photovoltaic; boost converter; VSC; MPPT

I. INTRODUCTION

Demographic changes and the development of certain geographical areas, suggest a significant increase in energy demand in the future. At this rate, in few decades, the fossil fuel reserves will not cover the needs of the world population. The first approach to this looming crisis is the reduction of energy consumption and in the meantime new clean and renewable energy sources should be used. In this regard, the sun, wind, biomass, ocean, etc. appear to be inexhaustible and easily exploitable energy. Among this wide variety of renewable energy sources, solar energy is considered as the most important renewable energy source which has gained increased attention in recent years. According to the International Energy Agency (IEA), an area of 145000 km² of photovoltaic (PV) is sufficient to cover the entire world's energy needs [1].

Standalone PV systems have been used for many years in various applications mainly in the residential and commercial sectors. When the generation of these off-grid PV systems exceeds the load demand, the surplus is generally stored in batteries for later use.

In recent years, the markets for grid-integrated PV applications are growing rapidly. Grid-tied PV systems can have considerable impact on the power system voltage, frequency and power flow. Advanced control of the

Voltage Source Converter (VSC) interfacing the PV system to the grid is the key technology to overcome both the power quality and grid stability challenges. The configuration of a grid connected PV system is illustrated in Fig.1.

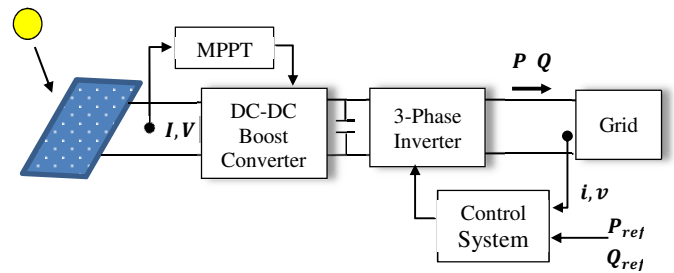


Fig. 1 Schematic diagram of PV-Grid system.

The basic inverter control schemes can be broadly divided into two categories: current control and voltage control. In grid-connected PV system, the inverter operates in current control mode where the grid regulates the voltage and frequency at the connection point by setting current reference for the inverter to allow exchange of real and reactive powers. The objective is to control the real and reactive power to some reference values [3], [4]. The power references and the voltage references are then used to set the references for the current controllers. The inverter is supplied from a DC link capacitor interconnected to the PV power system via a DC-DC converter combined with a Maximum Power Point Tracking (MPPT) controller to extract the maximum power from the PV system. The optimum operating point is highly dependent on the connected load and parameters such as the temperature and irradiance.

In the mathematical model of the Pulse Width Modulation (PWM) inverter expressed in the d-q rotating frame there is an inherent coupling between the real and reactive components of the current which makes it difficult to regulate the power injected into the grid from the PV generation system. An effective decoupling strategy based on proportional-integral (PI) controllers is designed to eliminate the interaction between the two current components.

II. MODELING OF THE GRID-TIED PV SYSTEM

The overall control system is shown in Fig. 2.

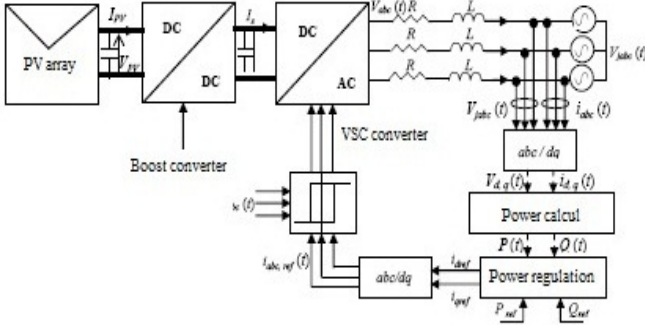


Fig. 2 Grid-tied PV inverter control system.

The principle of this control strategy is to convert the measured three phase currents and voltages into d-q values and then to calculate the current references and measured voltages as follow [5-6-7].

$$i_d^* = \frac{2P^*V_d - Q^*V_q}{3(V_d^2 + V_q^2)} \quad (1)$$

$$i_q^* = \frac{2P^*V_q - Q^*V_d}{3(V_d^2 + V_q^2)} \quad (2)$$

Where the * superscript denotes the reference quantities. V_d and V_q are the direct and quadratic components of the voltage measured at the connection point. I_d and I_q are the direct and quadratic current generated by PV system on the network. These currents are therefore dependent on the power required and the voltage measured at the connection point of the production. This measured voltage is transformed into the d-q reference frame before the current calculation.

A PLL is used to synchronize the Park transformation on the pulse of the voltage measured on the network. Thus, when the system is in a steady state, the direct component V_d leaving the Park transformation is a picture of the magnitude of the measured voltage and the quadratic component V_q is zero. Thus, equations (1-2) show I_d as a direct image of the active power and I_q as an image of the reactive power.

III. CONTROL SYSTEM DESIGN

A. P and Q Controller Design

Power flow control then consists of designing controllers to force the line currents to follow their references. It is desired that the VSC converter control system has a fast response with minimal interaction between the real and reactive power together with a strong damping of the resonance frequency. Two Proportional Integral (PI) controllers are used to regulate the active and reactive power. Since the design of the two control loops is similar, only the controller of the real power will be presented.

A simplified representation of the current control system is illustrated in Fig. 3.

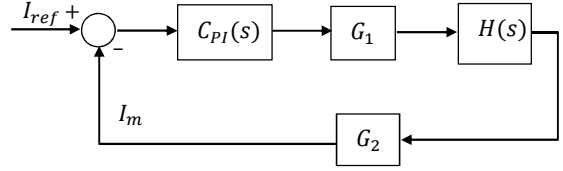


Fig.3 PI current control.

Considering $V_q = 0$ and V_d as constant.

$$G_1 = \frac{2}{3V_d} \quad \text{and} \quad G_2 = \frac{1}{G_1} = \frac{3V_d}{2} \quad (3)$$

$H(s)$ is the modeling of the dynamics of the VSC inverter.

$$H(s) = \frac{1}{1 + \tau s} \quad (4)$$

The conventional PI controller is given by

$$H(s) = \frac{K_p s + K_i}{s} \quad (5)$$

Where K_p and K_i are the proportional and integral gains respectively.

The transfer function of the closed loop system is second order

$$T(s) = \frac{G_1(K_p s + K_i)}{1 + \frac{G_1 G_2 K_p + 1}{K_i G_1 G_2} s + \frac{\tau}{K_i G_1 G_2} s^2} \quad (6)$$

And

$$\omega_n^2 = \frac{K_i G_1 G_2}{\tau} \cdot \frac{2\zeta}{\omega_n} = \frac{G_1 G_2 K_p + 1}{K_i G_1 G_2} \quad (7)$$

The same approach can be carried out for the reactive power controller design and the results will be identical.

B. DC Link Voltage Control

The voltage across the capacitor must be maintained at a fixed value. Neglecting the switching losses in the inverter as well as in the decoupling inductances, the relationship between the power absorbed by the active filter and the voltage across the capacitor is written as:

$$P_c = \frac{d}{dt} \left(\frac{1}{2} C V_{dc}^2 \right) \quad (8)$$

The block diagram of the V_{dc} control in a closed loop is presented in Fig. 4.

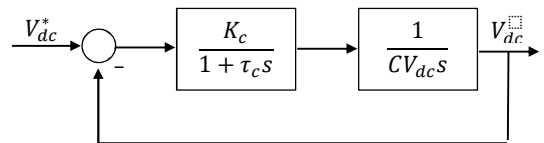


Fig.4 Block diagram of V_{dc} control.

The transfer function of the closed loop system is:

$$F_c(s) = \frac{1}{1 + \frac{2\zeta}{\omega_n} s + \frac{1}{\omega_n^2} s^2} \quad (9)$$

$$\omega_c = \sqrt{\frac{K_c}{CV_{dc}^* \tau_c}}$$

$$\zeta_c = \frac{1}{2} \sqrt{\frac{CV_{dc}^*}{K_c \tau_c}}$$

To achieve a closed-loop response with a good damping, we choose: $\zeta = 0.7$.

To removes the ripple voltage across the capacitor effect, we choose:

$$\tau_c = \frac{7}{2\pi \cdot 300} = 3.7 \cdot 10^{-3} \text{ sec}$$

For $V_{dc}^* = 600$ Vand $C = 0.0022$ F

$$K_c = \frac{CV_{dc}^*}{4\zeta_c^2 \cdot \tau_c} = 217.25$$

C. PLL Controller Design

The purpose of the PLL is to synchronize the current of the inverter with the voltage of the network. The diagram of block of the algorithm PLL implemented in the synchronous dq frame is presented in the Fig. 5.

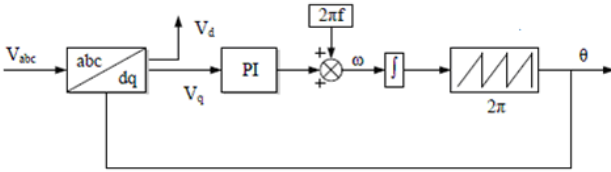


Fig. 5 PLL circuit.

The transfer function of the PLL circuit is given by:

$$H(s) = \frac{k_p s + \frac{k_p}{T_s}}{s^2 + k_p s + \frac{k_p}{T_s}} \quad (10)$$

We choose $T_s = 0.04$ and $\zeta = 1/\sqrt{2}$. Hence, the parameters of PI can be calculated as follows:

$$k_p = 2\zeta\omega_n = \frac{9.2}{T_s} \quad (11)$$

$$T_i = \frac{T_s \zeta^2}{2.3} \quad (12)$$

Where the natural frequency is given by:

$$\omega_n = \frac{4.6}{\zeta T_s} \quad (13)$$

IV. PERFORMANCE EVALUATION OF THE POWER CONTROLLERS

The model was implemented with Matlab and Simulink. Fig. 6 shows the active and reactive power flow responses for a step change in the reference of the real power. The VSC inverter controls the magnitude and angle of the AC voltage injected (Fig. 10). By varying the phase and magnitude of voltage injected power flow through the transmission line can be varied. Both Fig. 7 and 8 respectively shows the dynamic characteristics of three phases current and the voltage and current of the first phase at the connection point. The DC link voltage is shown in Fig. 9. These results show good tracking performance and transient responses of the two PI controllers.

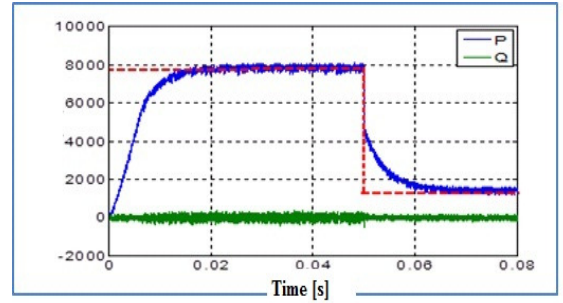


Fig.6 Active and Reactive power responses

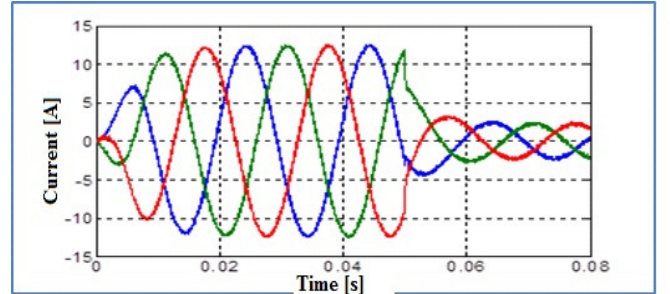


Fig.7 Currents waveforms

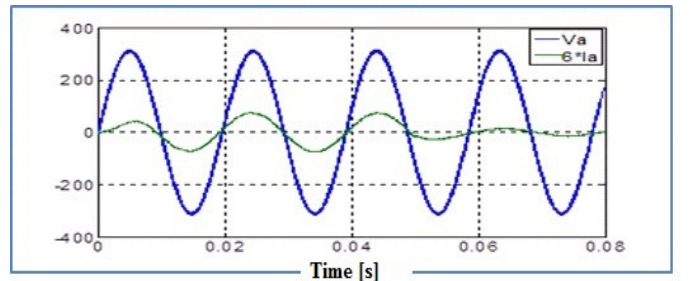


Fig. 8 Voltage and current of the first phase at the connection point.

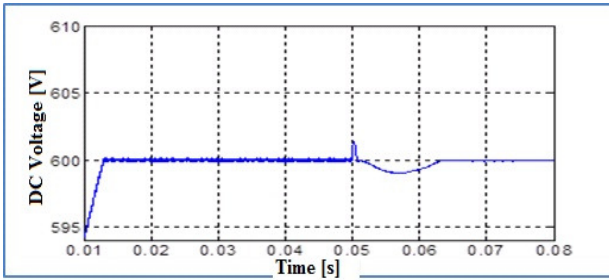


Fig. 9 DC voltage.

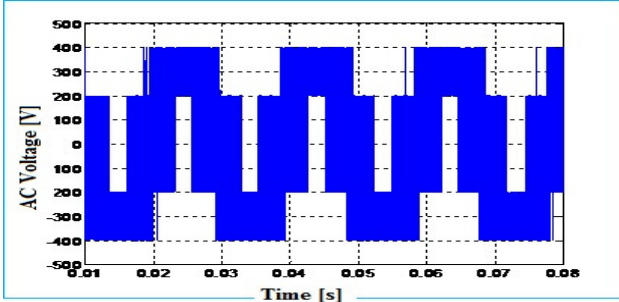


Fig.10 VSC voltage

V. IMPACT OF THE GPV SYSTEM ON THE GRID VOLTAGE

To show the effects of GPV in terms of voltage, consider the network model of Fig. 11. The network consists of three loads evenly spaced by 0.8 km consuming a total of 150 kW [8].

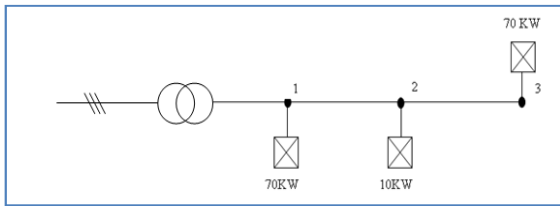


Fig.11. Network model used to study the impact of the inclusion of GPV.

Fig. 12 shows a positive impact of the inclusion of GPV on the voltage.

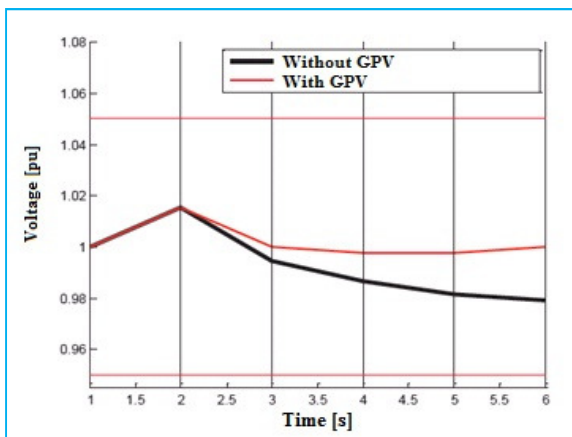


Fig.12. Example of a beneficial effect of the insertion of GPV in the test network.

In contrast, the insertion of GPV can cause power surges as shown in Fig. 13. A GPV of 700 KW is connected to node 3. Export of power causes an increase in the voltage that exceeds the permissible upper limit.

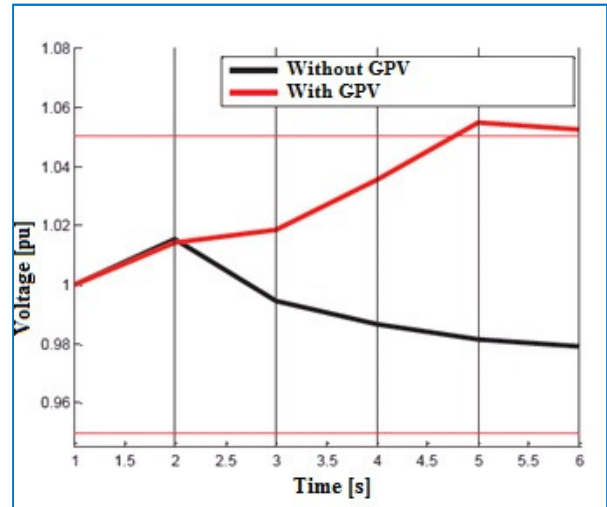


Fig.13 Example of voltage cause by inserting GPV.

VI. IMPACT OF THE GPV SYSTEM ON THE POWER FLOW

Connecting the GPV to the distribution network changes the power flow in the network. Consider the example of Fig. 11. The power flows obtained from this test without GPV network is illustrated in Fig. 14. Power flows are unidirectional from the upstream network and the transport network. The MV / LV transformer symbolises the border between the distribution network and the transport network.

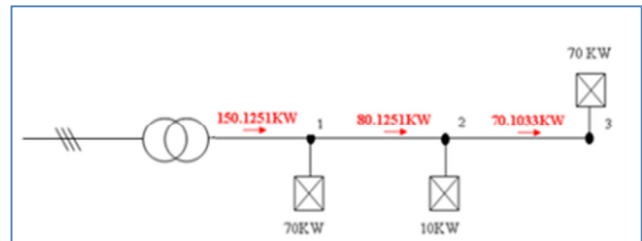


Fig.14 Power flow in the network without a GPV.

Let a GPV with a power of 100 KW be connected at node 2 as shown in the Fig. 15. It is assumed that the GPV operates at its maximum power. It will not only supply the load connected to the same node, but in addition, it will export power to other loads. Power flows then become bidirectional. Power from the distribution network is then 50.1032 KW. Moreover, in the previous case where the power came entirely from the upstream network, losses on the distribution system were 125.1 W. In the case of a GPV connected to node 2, the losses are reduced to 101.8 kW. The introduction of this GPV has reduced losses on the network.

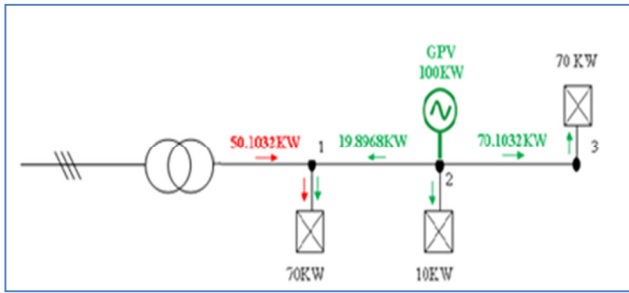


Fig.15 Power flow in the network test with GPV connected to node 2.

It can be concluded that with the power generated from the GPV, the transit of real power decreases and therefore the losses are reduces.

Depending on the number and size of GPV connected to the network can be in a position to export energy to the grid. Fig. 16 illustrates the case where power is exported to the grid when we connect, for example, a GPV of 100 KW to node 2 and a GPV of 100 KW to node 3.

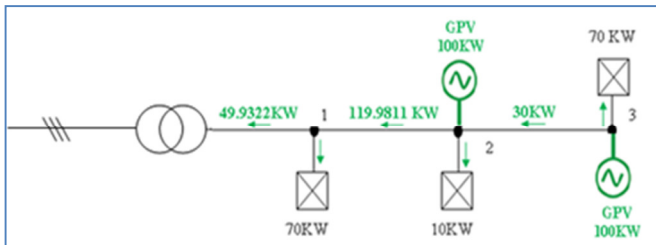


Fig.16. Example illustrating export power to the power grid.

VII. CONCLUSIONS

This simulation study has demonstrated the effectiveness of the decoupling strategy proposed allowing independent control of the real and reactive power flows in the network. The exchange of active and reactive power from distributed generation and grid can be controlled by the current output based on the power injected upstream at the connection point of the GPV. The results presented also demonstrate that energy production closer to consumers can reduce line losses. In contrast, the insertion of GPV can cause power surges. Before connecting a user must be studied in order to identify a solution that strictly necessary connection of the applicant while ensuring that this connection will have no effect on the operation of the network and the quality of the energy supplied to other users already connected.

REFERENCES

- [1] T. Akassewa, "Système d'alimentation Photovoltaïque avec stockage hybride pour l'habitat énergétiquement autonome", PhD Thesis, IAEM Lorraine, France, 2010.
- [2] T. Ackermann and V. Knyazkin, "Interaction between distributed generation and the distribution network: operation aspects", pages 1357-1362, 2002.
- [3] S. B. Kjaer, J. K. Pedersen, Blaabjerg "A review of singlephase grid-connected inverters for photovoltaic module", IEEE Trans Ind Appl, 2005; 41(5);pp:1292-1306.
- [4] P.S.Bimbhra, Power Electronics, Khanna publishers, Fourth edition, pp.127-198, 2012.
- [5] Moacyr A. G.de Brito, Leonardo P. Sampaio, Luigi G. Jr., Guilherme A. e. Melo, Carlos A. Canesin "Comparative analysis of MPPT techniques for PV applications", 2011 International Conference on Clean Electrical Power (ICCEP).
- [6] T. Allaoui, M. Denai and M. Bouhamida, "Decoupling Multivariable GPC Control of UPFC-Based Power Flow Compensation", Proc. 10th International Conference EPE-PEMC, Zagreb-Croatia, 2002.
- [7] M. Denai and T. Allaoui, "Adaptive fuzzy Decoupling of UPFC-Power Flow Compensation", Proc. 37th UPEC, Strathclyde University UK, 2002, pp. 9-11.
- [8] M. Sbaa, T. Allaoui, M. Denai and A. Chaker, "A robust adaptive fuzzy control of a unified power flow controller", Journal of Electric and Electronics Engineering, 2012.
- [9] J. G. Slootweg, W.L. Kling, "Impacts of distributed generation on power system transient stability", 2002 IEEE Power Engineering Society Summer Meeting, Chicago, US, July 2002.